Inorg. Chem. **2009**, *48*, 3617−3627

Acid-Sensitive Pt(II) 2,6-Di(pyridin-2-yl)pyrimidin-4(1*H*)-one Complexes

Hui Zhang,[†,‡] Bingguang Zhang,[†] Yunjing Li,[†] and Wenfang Sun*[,†]

Department of Chemistry and Molecular Biology, North Dakota State University, Fargo, North Dakota 58108-6050, and Coordination Chemistry Institute and State Key Laboratory, Nanjing University, Nanjing 210093, P.R. China

Received October 8, 2008

Three Pt(II) 2,6-di(pyridin-2-yl)pyrimidin-4(1*H*)-one complexes (**2**−**4**) with chloride or 4-ethynyltolyl ancillary ligands were synthesized and characterized. The photophysical properties of **2**−**4** were investigated in different solvents and at different acid concentrations. Their electronic absorption and emission responses at various acid concentrations were compared to those of **5**. **2**−**4** all exhibit a broad charge-transfer band in their electronic absorption spectra from 380 to 500 nm and emit at about 560 nm in acetonitrile at room temperature, presumably ascribed to the triplet metal-to-ligand charge transfer (^{3}MLCT) state. All of them exhibit broad and relatively strong triplet transient absorption in the visible to the near-IR region (450−820 nm). Upon addition of *p*-toluenesulfonic acid, the original charge-transfer band intensity decreases, accompanied by the increase of the absorption in the 350−400 nm region in their electronic absorption spectra. Meanwhile, the ^{3}MLCT emission is quenched, and the triplet transient absorption intensity decreases. The changes in electronic absorption, emission, and the transient absorption spectra are reversible upon the addition of base, that is, triethylamine. The reversible acid sensitivity is caused by the protonation and deprotonation of the carbonyl oxygen on the terdentate ligand. Therefore, these platinum complexes could be potential chromogenic and luminescent sensors for acids.

Introduction

Square-planar platinum(II) complexes exhibit intriguing photophysical properties[1] and potential applications in light-emitting devices,[2] photocatalysis,[3] nonlinear optical devices,[1d,f,4] and chemosensors.[5] In recent years, several studies on using platinum complexes as pH, cation, organic vapor, or biomolecule sensors have been reported.[5] The interests of using d^8 platinum(II) complexes for sensor application arise from their structural features and unique luminescence properties. First, the square-planar configuration of platinum complexes would allow for inter/intramolecular π-π and Pt−Pt interactions to occur at high concentrations or in the solid state. The degree of π-π and Pt−Pt interactions can be tuned when the complexes interact with H^+, metal cations, organic vapors, or biomolecules. This would change the electronic properties of the complexes, and thus, the UV−vis absorption and emission spectra would be varied. Second, many platinum terdentate complexes exhibit characteristic metal-to-ligand charge transfer (MLCT) absorption

* To whom correspondence should be addressed. E-mail: wenfang.sun@ndsu.edu.
† North Dakota State University.
‡ Nanjing University.

(1) (a) Lai, S.-W.; Chan, M. C. W.; Cheung, K.-K.; Che, C.-M. *Inorg. Chem.* **1999**, *38*, 4262. (b) Yam, V. W.-W.; Tang, R. P.-L.; Wong, K. M.-C.; Cheung, K.-K. *Organometallics* **2001**, *20*, 4476. (c) Yang, Q.-Z.; Wu, L.-Z.; Wu, Z.-X.; Zhang, L.-P.; Tung, C.-H. *Inorg. Chem.* **2002**, *41*, 5653. (d) Sun, W.; Wu, Z.-X.; Yang, Q.-Z.; Wu, L.-Z.; Tung, C.-H. *Appl. Phys. Lett.* **2003**, *82*, 850. (e) Lu, W.; Mi, B. X.; Chan, M. C. W.; Hui, Z.; Che, C. M.; Zhu, N.; Lee, S. T. *J. Am. Chem. Soc.* **2004**, *126*, 4958. (f) Guo, F.; Sun, W.; Liu, Y.; Schanze, K. *Inorg. Chem.* **2005**, *44*, 4055. (g) Shao, P.; Sun, W. *Inorg. Chem.* **2007**, *46*, 8603.

(2) (a) Chassot, L.; von Zelewsky, A.; Sandrini, D.; Maestri, M.; Balzani, V. *J. Am. Chem. Soc.* **1986**, *108*, 6084. (b) Yersin, H.; Donges, D.; Humbs, W.; Strasser, J.; Sitters, R.; Glasbeek, M. *Inorg. Chem.* **2002**, *41*, 4915. (c) Kwok, C.-C.; Ngai, H. M. Y.; Chan, S.-C.; Sham, I. H. T.; Che, C.-M.; Zhu, N. *Inorg. Chem.* **2005**, *44*, 4442.

(3) (a) van der Boom, M. E.; Milstein, D. *Chem. Rev.* **2003**, *103*, 1759. (b) Dick, A. R.; Kampf, J. W.; Sanford, M. S. *Organometallics* **2005**, *24*, 482.

(4) (a) Guo, F.; Sun, W. *J. Phys. Chem. B* **2006**, *110*, 15029. (b) Sun, W.; Zhu, H.; Barron, P. M. *Chem. Mater.* **2006**, *18*, 2602. (c) Shao, P.; Li, Y.; Sun, W. *J. Phys. Chem. A.* **2008**, *112* (6), 1172.

(5) (a) Wong, K.-H.; Chan, M. C.-W.; Che, C. M. *Chem.−Eur. J.* **1999**, *5*, 2845. (b) Yang, Q.-Z.; Wu, L.-Z.; Zhang, H.; Chen, B.; Wu, Z.-X.; Zhang, L.-P.; Tung, Z.-H. *Inorg. Chem.* **2004**, *43*, 5195. (c) Wong, K. M.-C.; Tang, W.-S.; Lu, X.-X.; Zhu, N.; Yam, V. W.-W. *Inorg. Chem.* **2005**, *44*, 1492. (d) Han, X.; Wu, L.-Z.; Si, G.; Pan, J.; Yang, Q.-Z; Zhang, L.-P.; Tung, C.-H. *Chem.−Eur. J.* **2007**, *13*, 1231. (e) Lo, H.-S.; Yip, S.-K.; Wong, K. M.-C.; Zhu, N.; Yam, V. W.-W. *Organometallics* **2006**, *25*, 3537. (f) Wong, K. M.-C.; Tang, W.-S.; Chu, B. W.-K.; Zhu, N.; Yam, V. W.-W. *Organometallics.* **2004**, *23*, 3459. (g) Kui, S. C. F.; Chui, S. S.-Y.; Che, C.-M.; Zhu, N. *J. Am. Chem. Soc.* **2006**, *128*, 8297. (h) Wong, K. M.-C.; Yam, V. W.-W. *Coord. Chem. Rev.* **2007**, *251*, 2477.

10.1021/ic801919g CCC: $40.75
Published on Web 03/16/2009

Scheme 1. Synthetic Route and Structures of Complexes **1**−**5**

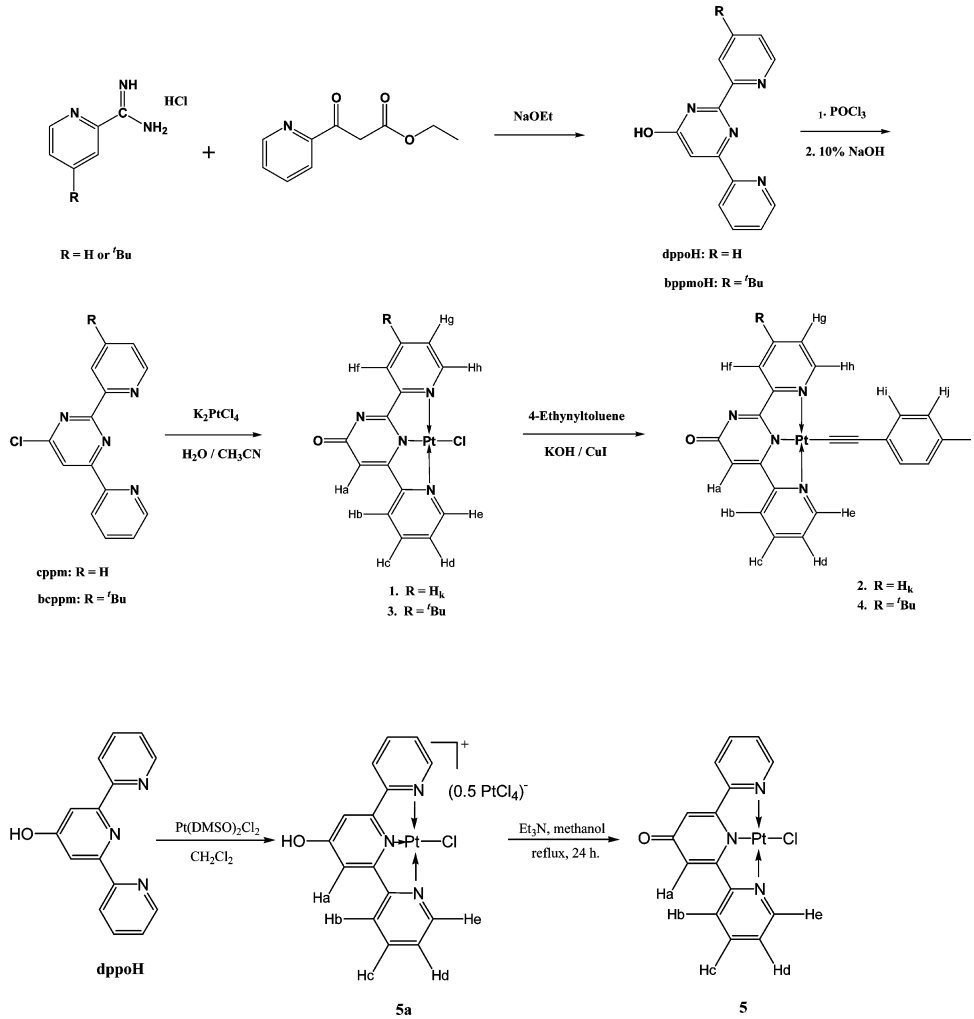

in the visible spectral region, and long-lived ^{3}MLCT emission in the visible to near-IR region in solutions and solids at room temperature. The ^{1}MLCT absorption and ^{3}MLCT emission energies could be tuned by the different chemical environments. To respond to the chemical environment, such as pH change or cations, respective proton-receptors or cation-binding units need to be introduced either on the monodentate coligand or on the terdentate ligand. For example, for cations sensing, crown ethers have been used as binding units;[5b,e] and for pH sensing, amino-substituted platinum complexes have been studied.[5c,d] Although the studies reported in the literature are quite intriguing, most of the platinum(II) complex based pH sensors studied so far are based on the protonation of the amino substituent,[5c,d,6] which switches on the ^{3}MLCT emission that was quenched by photoinduced electron transfer (PET) prior to protonation. To date, no platinum complexes with a proton receptor other than an amino substituent have been reported.

To explore the possibility of utilizing other functional groups as proton receptors, our group recently synthesized several platinum complexes with a carbonyl functional group on the terdentate ligand, which could potentially serve as a proton-accepting site. The synthetic route and the structures of the new platinum complexes are shown in Scheme 1. Complexes **3** and **4** are the analogues of complexes **1** and **2**, respectively, which contain a *tert*-butyl substituent to increase the solubility of the complexes in organic solvents. Complex **5** is a known complex reported in a Japanese Patent,[7] which is synthesized for comparison purpose to distinguish whether the proton-accepting site is the carbonyl oxygen or the 3-nitrogen atom at the pyrimidin-4(1*H*)-one ring. The photophysical properties of **2**−**5** and the acid-sensing behaviors of **2**−**5** have been systematically investigated and reported in this paper.

Experimental Section

Synthesis. The ligands 4-chloro-2,6-bis(2-pyridyl)pyrimidine (cppm)[8] and 2,6-di(2-pyridyl)-4(1*H*)-pyridone (dppo),[9] as well as the precursors 2-amidino-4-*tert*-butylpyridine hydrochloride[7] and ethyl 3-oxo-3-(2-pyridinyl)propanoate,[10] were synthesized according to the procedures reported in the literature. The ligand 2-(4-*tert*-butylpyridin-2-yl)-4-chloro-6-(pyridin-2-yl)pyrimidine (bcppm) and its precursor 2-(4-*tert*-butylpyridin-2-yl)-6-(pyridin-2-yl)pyrimidin-4-ol (bppmoH), as well as the Pt(II) complexes **1**−**4** are new

(6) Wong, K. M.-C.; Yam, V. W.-W. *Coord. Chem. Rev.* **2007**, *251*, 2477.

(7) Yagi, S.; Akiyama, S.; Iida, K. *Jpn. Kokai Tokkyo Koho*, Japan Patent: JP2007231008, **2007**.

(8) Lafferty, J. J.; Case, F. *J. Org. Chem.* **1967**, *32*, 1591.

(9) Potts, K. T.; Konwar, D. *J. Org. Chem.* **1991**, *56*, 4815.

(10) Alves, M. J.; Fortes, A. G.; Lemos, A.; Martins, C. *Synthesis.* **2005**, 555.

compounds/complexes. The synthetic procedures and the characterization data are thus provided in the following Experimental Section. Although **5** is a known complex, its characterization data has not been reported in the literature. Additionally, we used a different procedure to synthesize **5** from deprotonation of [Pt(dppoH)Cl]·0.5($PtCl_4$) (**5a**). Therefore, the synthesis and characterization of **5** are also reported in this paper. All the starting chemicals were purchased from Alfa Aesar. All solvents were analytical grade and used as received unless otherwise stated.

^{1}H NMR spectra were measured on a Varian 500 MHz VNMR spectrometer. ESI-HRMS analyses were conducted on a Bruker Daltonics BioTOF III mass spectrometer. Elemental analyses were conducted by NuMega Resonance Laboratories Inc., San Diego, CA.

2-(4-*tert*-Butylpyridin-2-yl)-6-(pyridin-2-yl)pyrimidin-4-ol (bppmoH). A mixture of ethyl 3-oxo-3-(2-pyridinyl)propanoate (1.93 g, 0.01 mol), NaOEt (0.68 g, 0.01 mol), 2-amidino-4-*tert*-butylpyridine hydrochloride (2.14 g, 0.01 mol), and 40 mL of absolute ethanol was stirred at reflux for 3 h, followed by stirring at room temperature for overnight. The resultant mixture was concentrated to about 10 mL and then diluted with water. The precipitate was recrystalized from ethanol and water to afford 1.10 g of a light red solid product (yield: 35%). ^{1}H NMR ($CDCl_3$) δ: 8.75 (d, 1H, J = 4.0 Hz), 8.61 (m, 2H), 8.48 (d, 1H, J = 8.0 Hz), 7.92 (dt, 1H, J = 7.5, 1.5 Hz), 7.60 (s, 1H), 7.52 (dd, 1H, J = 5.0, 2.0 Hz), 7.41−7.44 (m, 1H), 1.47 (s, 9H) ppm.

2-(4-*tert*-Butylpyridin-2-yl)-4-chloro-6-(pyridin-2-yl)pyrimidine (bcppm). A mixture of bppmoH (1.63 g, 5.30 mmol) and 15 mL of $POCl_3$ was stirred at reflux for 2 h. The excess $POCl_3$ was then removed under reduced pressure, and the residues were neutralized (pH∼7) with 10% sodium hydroxide aqueous solution and extracted with ether. After that, the ether was removed under reduced pressure, and the residues were recrystalized from hexane to afford 1.09 g of a light brown product (yield: 63%). ^{1}H NMR ($CDCl_3$) δ: 8.81 (d, 1H, J = 5.0 Hz), 8.77 (d, 1H, J = 4.5 Hz), 8.70 (d, 1H, J = 8.0 Hz), 8.63 (d, 1H, J = 1.5 Hz), 8.46 (s, 1H), 7.95 (dt, 1H, J = 7.5, 1.5 Hz), 7.46−7.50 (m, 2H), 1.45 (s, 9H) ppm.

1. 1 was synthesized by a slight modification of the literature procedure.[1a] A stirred mixture of K_2PtCl_4 (415 mg, 1.0 mmol) and cppm (283 mg, 1.0 mmol) in CH_3CN/H_2O (25/25 mL) was heated to reflux under N_2 for 24 h. The yellow precipitate was collected by filtration, washed with water and acetonitrile, and dried in vacuum. A 220 mg quantity of a yellow product was obtained (yield: 46%). Because of the poor solubility of **1** in organic solvent, NMR data for this complex was unable to be obtained. However, ESI-MS analysis confirmed the formation of this complex. ESI-MS: m/z calcd for $[C_{14}H_9ClN_4NaOPt^{194}]^+$ 501.0, found 501.1 (81%); calcd for $[C_{14}H_9ClN_4NaOPt^{195}]^+$ 502.0, found 502.1 (100%); calcd for $[C_{14}H_9ClN_4NaOPt^{196}]^+$ 503.0, found 503.1 (98%).

2. 2 was synthesized by modification of the literature procedure.[1f] Potassium hydroxide (20 mg, 0.36 mmol) was added to a 100 mL DMF solution of 4-ethynyltoluene (28 mg, 0.24 mmol), and the mixture was stirred at room temperature for 0.5 h. Complex **1** (107 mg, 0.20 mmol) and CuI (5 mg, 0.026 mmol) were then added to the reaction mixture. The resultant solution was stirred at room temperature for 24 h., followed by stirring at 70 °C for another 24 h under a N_2 atmosphere. The reaction mixture was filtered, and the orange filtrate was concentrated to about 5 mL under reduced pressure. Then 50 mL of water was added, and the precipitate was collected by filtration and washed with hexane and water. Recrystalization from dichloromethane and acetonitrile afforded 83 mg of a red solid product (yield: 62%). ^{1}H NMR (DMSO-d_6) δ: 9.11 (d, 1H, J = 5.5 Hz, H_h), 9.05 (d, 1H, J = 5.5 Hz, H_e), 8.38 (m, 3H, H_c, H_f and H_k), 8.14 (br. s, 1H, H_b), 7.86 (t, 1H, J = 6.5 Hz, H_g), 7.77 (t, 1H, J = 6.0 Hz, H_d), 7.36 (d, 2H, J = 8.0 Hz, H_i), 7.13 (d, 2H, J = 7.5 Hz, H_j), 6.90 (s, 1H, H_a), 3.32 (s, 3H) ppm. ESI-MS: m/z calcd for $[C_{23}H_{17}N_4OPt^{194}]^+$ 559.1024, found 559.1033 (74%); calcd for $[C_{23}H_{17}N_4OPt^{195}]^+$ 560.1047, found 560.1071 (100%); calcd for $[C_{23}H_{17}N_4OPt^{196}]^+$ 561.1055, found 561.1062 (74%). Anal. Calcd for $C_{23}H_{16}N_4OPt\cdot CH_2Cl_2\cdot 2H_2O$: C, 42.36; H, 3.26; N, 8.23. Found: C, 42.03; H, 2.87; N, 8.56.

3. 3 was synthesized by modification of the literature procedure.[1a] A stirred mixture of K_2PtCl_4 (415 mg, 1 mmol) and bcppm (283 mg, 1 mmol) in CH_3CN/H_2O (25/25 mL) was heated at reflux for 24 h. to yield a red solution, which was evaporated under reduced pressure to remove most of the solvent to afford the crude product. The precipitate was collected by filtration, and then recrystalized in about 30 mL of acetonitrile and dichloromethane (V/V = 1:1) mixture. The orange solid collected was washed with hexane and dried under vacuum. A 220 mg quantity of pure product was obtained (yield: 37%). ^{1}H NMR (DMSO-d_6) δ: 8.93 (d, 1H, J = 5.0 Hz, H_h), 8.76 (d, 1H, J = 6.0 Hz, H_e), 8.47 (d, 1H, J = 7.0 Hz, H_g), 8.42 (t, 1H, J = 7.0 Hz, H_c), 8.06 (s, 1H, H_f), 7.98 (d, 1H, J = 3.0 Hz, H_b), 7.85 (t, 1H, J = 6.5 Hz, H_d), 7.09 (s, 1H, H_a), 1.40 (s, 9H) ppm. ESI-MS: m/z calcd for $[C_{18}H_{18}ClN_4OPt^{194}]^+$ 535.0790, found 535.0787 (78%); calcd for $[C_{18}H_{18}ClN_4OPt^{195}]^+$ 536.0813, found 536.0822 (90%); calcd for $[C_{18}H_{18}ClN_4OPt^{196}]^+$ 537.0806, found 537.0815 (100%). Anal. Calcd for $C_{18}H_{17}ClN_4OPt$: C, 40.34; H, 3.20; N, 10.46. Found: C, 40.19; H, 2.70; N, 10.61.

4. The synthesis of **4** followed the procedure described for the synthesis of **2**, except that **3** instead of **1** was used as the precursor and the crude product was recrystalized from dichloromethane and hexane. A red solid was obtained as the product (yield: 65%). ^{1}H NMR ($CDCl_3$) δ: 9.31 (d, 1H, J = 5.0 Hz, H_h), 9.05 (d, 1H, J = 6.0 Hz, H_e), 8.35 (s, 1H, H_f), 8.16 (t, 1H, J = 7.0 Hz, H_c), 7.89 (d, 1H, J = 8.0 Hz, H_g), 7.52 (m, 2H, H_b and H_d), 7.42 (d, 2H, J = 8.0 Hz, H_i), 7.15 (d, 2H, J = 8.0 Hz, H_j), 6.73 (s, 1H, H_a), 2.39 (s, 3H), 1.42 (s, 9H) ppm. ESI-MS: m/z calcd for $[C_{27}H_{25}N_4OPt^{194}]^+$ 615.1650, found 615.1686 (65%); calcd for $[C_{27}H_{25}N_4OPt^{195}]^+$ 616.1673, found 616.1701 (100%); calcd for $[C_{27}H_{25}N_4OPt^{196}]^+$ 617.1682, found 617.1710 (70%). Anal. Calcd for $C_{27}H_{24}N_4Opt\cdot 1.5H_2O$: C, 50.46; H, 4.23; N, 8.72. Found: C, 50.45; H, 4.17; N, 8.97.

[Pt(dppoH)Cl]·0.5($PtCl_4$) (5a). A mixture of $Pt(DMSO)_2Cl_2$ (422 mg, 1 mmol), dppoH (249 mg, 1 mmol), and 40 mL of dichloromethane was stirred at reflux under N_2 for 8 h, followed by stirring at room temperature for 24 h. During the reaction, a yellow solid precipitated. The precipitate was collected by filtration and washed with dichloromethane. A 420 mg quantity of product was obtained (yield: 86%). ^{1}H NMR (DMSO-d_6) δ: 8.94 (d, 2H, J = 5.5 Hz, H_e), 8.52 (d, 2H, J = 7.5 Hz, H_b), 8.48 (t, 2H, J = 7.5 Hz, H_c), 7.93 (t, 2H, J = 6.0 Hz, H_d), 7.87 (s, 2H, H_a) ppm. Anal. Calcd for $C_{15}H_{11}ClN_3OPt\cdot 0.5PtCl_4\cdot CH_2Cl_2$: C, 26.21; H, 1.79; N, 5.73. Found: C, 25.96; H, 2.13; N, 5.40.

5. A mixture of **5a** (293 mg, 0.4 mmol), triethylamine (1 mL) and 50 mL methanol was stirred at reflux under N_2 for 24 h. The solid was collected by filtration, washed with water, and recrystallized from methanol and ether. A 110 mg quantity of a brownish yellow solid product was obtained (yield: 55%). ^{1}H NMR (DMSO-d_6) δ: 8.86 (d, 2H, J = 5.5 Hz, H_e), 8.31 (t, 2H, J = 7.5 Hz, H_c), 8.26 (d, 2H, J = 7.5 Hz, H_b), 7.73 (t, 2H, J = 6.5 Hz, H_d), 7.03 (s, 2H, H_a) ppm. ESI-MS: m/z calcd for $[C_{15}H_{11}ClN_3OPt^{194}]^+$ 478.0211, found 478.0228 (76%); calcd for $[C_{15}H_{11}ClN_3OPt^{195}]^+$ 479.0234, found 479.0243 (92%); calcd for $[C_{15}H_{11}ClN_3OPt^{196}]^+$ 480.0226,

found 480.0234 (100%). Anal. Calcd for $C_{15}H_{10}ClN_3OPt \cdot 0.5H_2O$: C, 36.93; H, 2.27; N, 8.61. Found: C, 36.70; H, 2.25; N, 8.44.

Photophysical Measurements. All of the photophysical measurements were carried out in acetonitrile solutions unless otherwise noted. The electronic absorption spectra were measured on a UV-2501 PC UV−visible spectrophotometer in a 1 cm quartz cuvette. For the solvent-dependent UV−vis absorption measurements, because of the poor solubility of **2**−**4** in toluene, methanol, and dichloromethane, the complexes were initially dissolved in DMSO to prepare a concentrated mother solution, then the DMSO solution was diluted with corresponding solvents (for **3**, its acetonitrile solution was also prepared by the same method). Because the percentage of DMSO in the diluted solutions is no more than 5%, the effects of DMSO could presumably be neglected. Steady state emission spectra were measured on a FP-6500 spectrofluorometer or a SPEX Fluorolog-3 fluorometer/phosphorometer. The emission quantum yields were determined by the comparative method,[11] and a degassed aqueous solution of $[Ru(bpy)_3]Cl_2$ ($\Phi_{em} = 0.042$ at 436 nm excitation)[12] was used as the reference. The emission lifetimes, the triplet excited-state quantum yields, and the triplet transient different absorption spectra were measured on an Edinburgh Instruments LP920 laser flash photolysis spectrometer. The excitation source was the third harmonic output (355 nm) of a Quantel Brilliant Nd:YAG laser (pulse width ~ 4.1 ns), and the repetition rate was adjusted to 1 Hz. All the sample solutions were purged with argon for 25 min before each measurement.

The molar extinction coefficient of the triplet excited state ($\varepsilon_{T1\text{-}Tn}$) and triplet quantum yield (Φ_T) were determined by the partial saturation method,[13] which has been described previously.[4c] The optical density at the absorption band maximum, namely 725 nm for **2** and **4**, 460 nm for **3**, and 770 nm for **5** was monitored when the excitation energy at 355 nm was gradually increased. The experimental data was then fitted by eq 1 to obtain the ε_T and Φ_T.[13]

$$\Delta OD = a(1 - \exp(-bI_p)) \quad (1)$$

where ΔOD is the optical density at the band maximum, I_p is the pump intensity in Einstein cm^{-2}, $a = (\varepsilon_T - \varepsilon_0)dl$, and $b = 2303\varepsilon_0^{ex}\Phi_T/A$. ε_T and ε_0 are the absorption coefficients of the excited state and the ground state at the band maximum, respectively, ε_0^{ex} is the ground-state absorption coefficient at the excitation wavelength of 355 nm, d is the concentration of the sample (mol L^{-1}), l is the thickness of the sample, and A is the area of the sample irradiated by the excitation beam.

Results and Discussion

Synthesis and Characterization. The synthesis of the platinum chloride complexes **1** and **3** used 2-(4-*R*-pyridin-2-yl)-4-chloro-6-(pyridin-2-yl)pyrimidine instead of 2-(4-*R*-pyridin-2-yl)-6-(pyridin-2-yl)pyrimidin-4-ol as the precursor because purification of 2-(4-*R*-pyridin-2-yl)-6-(pyridin-2-yl)pyrimidin-4-ol was difficult. After conversion of the −OH substituent to the −Cl substituent, the resultant 2-(4-*R*-pyridin-2-yl)-4-chloro-6-(pyridin-2-yl)pyrimidine was much easier to be purified through recrystalization. When 2-(4-*R*-pyridin-2-yl)-4-chloro-6-(pyridin-2-yl)pyrimidine reacted with K_2PtCl_4 in a CH_3CN/H_2O mixture, ligand complexation and hydrolysis that converted −Cl to −OH, as well as the isomerization of pyrimidin-4-ol ring to pyrimidin-4(1*H*)-one occurred simultaneously. Because of the poor solubility of **1**, it was used directly for the reaction of **2** without further purification. Thus, spectroscopic characterization of **1** was unable to be carried out except for that mass spectrometry confirmed the formation of **1**. After conversion of the chloride ligand to 4-ethynyltolyl ligand, the solubility of **2** in CH_3CN, DMSO and DMF was improved. To improve the solubility of **1**, another attempt was conducted to introduce a *tert*-butyl substituent to the 4-position of the 2-pyridyl ring to reduce the intermolecular π-π stacking. This resulted in the complex **3**. Substitution of −Cl by 4-ethynyltolyl gave rise to complex **4** that has further improved solubility in CH_3CN. The structures of **2**−**4** were confirmed by ^1H NMR, HRMS, and elemental analysis. Assignment of the ^1H NMR resonance peaks at the downfield to the corresponding protons is based on the chemical environment and their splitting patterns. The chemical shifts for the protons at the 2-pyridyl ring (H_f, H_g, H_h for **3** and **4**, and H_f, H_g, H_h, H_k for **2**) appear at lower field compared to their corresponding protons at the 6-pyridyl ring (H_b−H_e). This should be due to the stronger electron-withdrawing effect of the two nitrogens on the pyrimidin-4(1*H*)-one ring on the 2-pyridyl ring in comparison to that on the 6-pyridyl ring, which deshields the protons on the 2-pyridyl ring more than those on the 6-pyridyl ring. On each of the pyridyl ring, the protons at the *ortho*-positions (i.e., H_e and H_h) of the N are more deshielded than the protons at the *para*-position of the N (i.e., H_c and H_k); and the protons at the *ortho*-position (H_b, H_d, H_g, H_f) of N are the least deshielded ones compared to the protons at the *ortho*- and *para*-positions of the same ring. The most important feature on the ^1H NMR spectra of **2**−**4** is the chemical shift for H_a, which appears around or below 7.0 ppm as a singlet. This chemical shift is in line with the chemical shift of the corresponding proton on 4(3*H*)-pyrimidinone,[14] indicating that the dominant form of the terdentate ligand is the 2,6-di(pyridin-2-yl)pyrimidin-4-one, not the 2,6-di(pyridin-2-yl)pyrimidin-4-ol. If the latter is the case, the chemical shift for H_a would shift to lower field because of the aromatic anisotropy deshielding effect, which has been evident from the chemical shift of H_a in **5a** (displayed in Figure 1). Another piece of evidence supporting the 2,6-di(pyridin-2-yl)pyrimidin-4-one form arises from the reported crystal structure of *cis*-diammine(1-methylcytosine-N3)(thyminato-N1)platinum(II) perchlorate, in which the bond lengths for the two carbon−oxygen bonds on the thyminato ring are 1.22 and 1.25 Å, confirming that it is a double bond between carbon and oxygen atoms.[15] Although the structures of **2**−**4** are not exactly the same as that of *cis*-diammine(1-methylcytosine-N3)(thyminato-N1)platinum-(II) perchlorate, the reported crystal structure still provides a strong implication of the pyrimidin-4-one form rather than the pyrimidin-4-ol form in complexes **2**−**4**.

(11) Demas, J. N.; Crosby, G. A. *J. Phys. Chem.* **1971**, *75*, 991.
(12) Van Houten, J.; Watts, R. J. *J. Am. Chem. Soc.* **1976**, *98*, 4853.
(13) Carmichael, I.; Hug, G. L. *J. Phys. Chem. Ref. Data* **1986**, *15*, 1.
(14) http://riodb01.ibase.aist.go.jp/sdbs/cgi-bin/direct_frame_top.cgi (accessed Jan 20, 2009).
(15) Faggiani, R.; Lippert, B.; Lock, C. J. L.; Pfab, R. *Inorg. Chem.* **1981**, *20*, 2381.

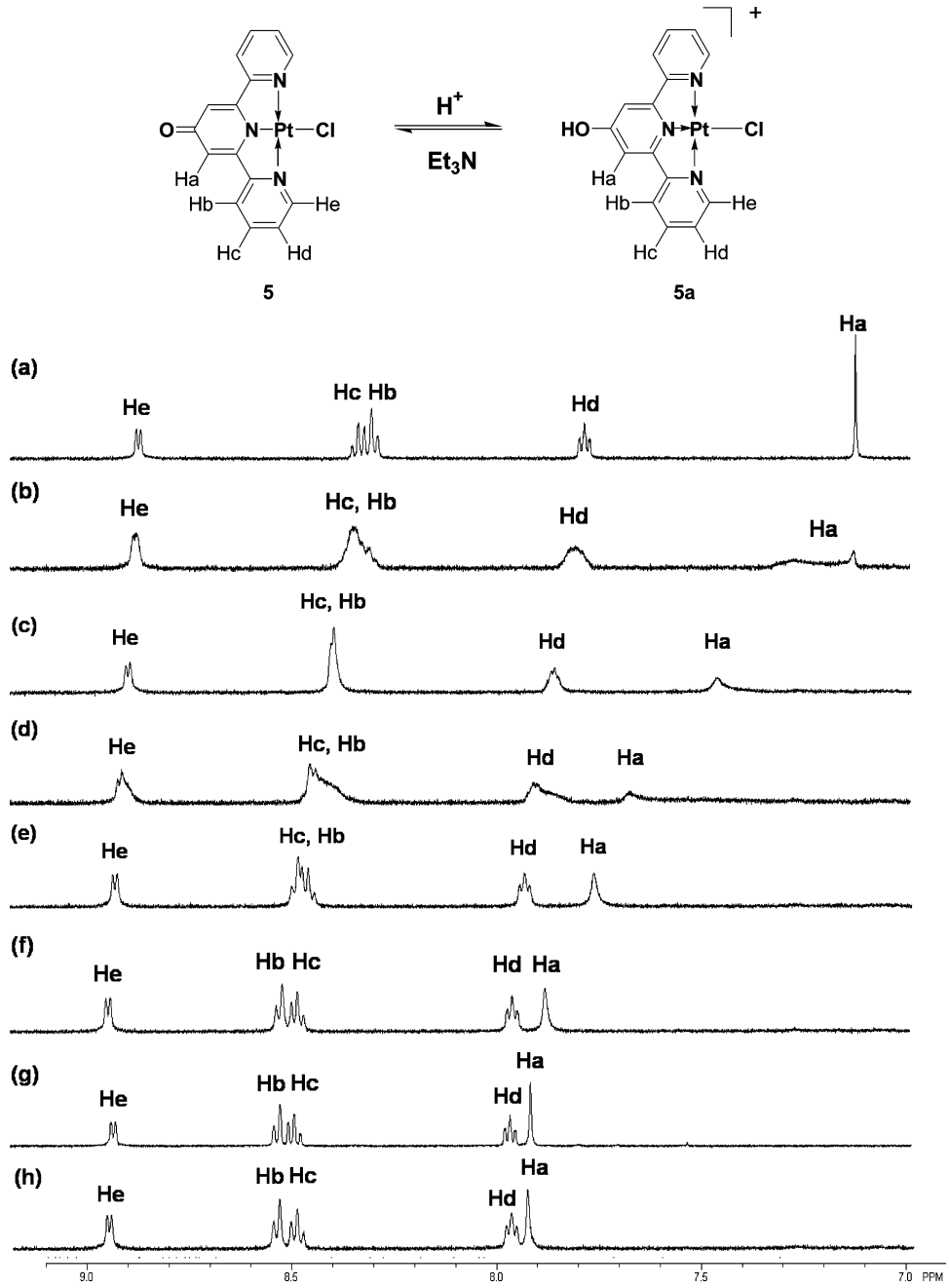

Figure 1. ^{1}H NMR spectra of **5** with (a) 0, (b) 0.2, (c) 0.4, (d) 0.6, (e) 0.8, (f) 1.0, and (h) 1.2 equiv of CF_3COOH in DMSO-d_6, respectively. (g) Spectrum of **5a** in DMSO-d_6.

Complex **5** was obtained by deprotonation of **5a** under basic conditions. The structures of **5a** and **5** were confirmed through ^{1}H NMR, HRMS, and elemental analysis. As displayed in panels a and g of Figure 1, the chemical shifts of the protons on **5a** (shown in Figure 1g) are all downfield shifted compared to the corresponding protons on **5** (shown in Figure 1a), which should be due to the aromatic anisotropy deshielding of the pyridine-4-ol ring. The most drastic change was observed for proton H_a, with a chemical shift of 7.03 ppm for **5** and 7.87 ppm for **5a**. Considering the similarity of the chemical shifts of H_a in **2**−**4** to that of **5**, we further confirm that the dominant form for the middle ring of the terdentate ligand is pyrimidin-4-one, not pyrimidin-4-ol. Thus, obtaining both **5a** and **5** is critical because it not only helps us to identify the structures of the complexes **2**−**4**, but also will aid our understanding of the mechanism when protonation of **5** occurs, which will be discussed later.

The structures of **5** and **5a** have also been supported by their IR spectra. As shown in the Supporting Information Figure S1, the IR spectrum of **5a** exhibits two peaks at 3190 cm^{-1} and 1216 cm^{-1}, which are absent in the spectrum of **5** and can be attributed to H-bonded OH stretching and C−O stretching. In contrast, the IR spectrum of **5** shows a peak at 1530 cm^{-1}, which can be ascribed to the C═O stretching. The much lower stretching frequency of C═O could be partially due to the conjugation with two C═C bonds. On the other hand, such a low frequency also indicates that the middle ring could not be 100% pyridin-4-one form; it should

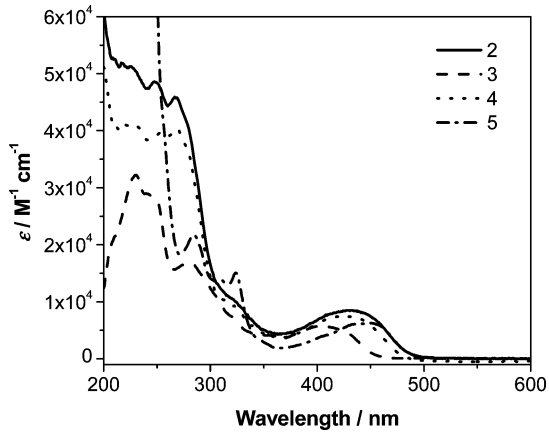

Figure 2. Electronic absorption spectra of **2**−**5**. **2**− **4** are in acetonitrile, and **5** is in acetonitrile + 5% DMSO.

be a resonance form between pyridine-4-one and pyridine-4-ol but with the pyridine-4-one form as the dominant one.

Electronic Absorption Spectra. Figure 2 shows the electronic absorption spectra of complexes **2**−**5** in acetonitrile, and the band maxima and extinction coefficients are presented in Table 1. The UV−vis absorptions of **2**−**5** follow Beer's law in the concentration range of 5.0×10^{-6} to 5.0×10^{-5} mol/L, indicating that no aggregation occurs in this concentration range.

All complexes exhibit intense absorption below 350 nm, which can be assigned to the intraligand $^1\pi$, π^* transition.[1a] The broadband from 380 to 500 nm is attributed to the ^{1}MLCT transition, likely mixed with some ligand-to-ligand charge transfer (^{1}LLCT) from the 4-ethnyltolyl ligand to the terdentate ligand in the case of **2** and **4**. This feature has been suggested by Yam and co-workers and supported by density functional theory (DFT) calculation for platinum terpyridyl phenylacetylide complexes.[1b,16] Because of the involvement of the ^{1}LLCT transition that appears at lower energy, and the decrease of the ^{1}MLCT transition energy in the presence of electron-donating 4-ethnyltolyl ligand,[1b,5b] the charge-transfer band maxima for **2** and **4** are red-shifted to ~430 nm compared to that of **3** (~405 nm). The UV−vis absorption spectra of **2** and **4** are quite similar, indicating the minor effect of the *tert*-butyl substituent on the electronic absorption.

The charge transfer nature of the low-energy absorption band for **2**−**5** was further verified by the solvent-dependent electronic absorption measurements. As displayed in Figure 3 for **3** and **4**, and Supporting Information Figure S2 for **2**, the low-energy absorption bands of **2**−**4** are sensitive to the polarity of the solvent. Low-polarity solvents, such as toluene and CH_2Cl_2, cause a bathochromic shift of the low-energy band compared to that in more polar solvents, such as DMSO, CH_3OH, and CH_3CN. The negative solvatochromic effect has been commonly seen in many platinum terpyridyl complexes.[1]

A point worthy of mention is that in comparison to the charge transfer band of 2,6-di(pyridin-2-yl)pyrimidin-4(1*H*)-one Pt(II) chloride complex **3**, the corresponding band of 2,6-di(pyridin-2-yl)pyridin-4(1*H*)-one Pt(II) chloride complex **5** is significantly red-shifted. This reflects the influence of the different electronic structures of the middle pyrimidin-4-one ring and the pyridine-4-one ring in their respective terdentate ligand. The UV−vis spectra of 2,6-bis(2-pyridyl)pyrimidin-4-ol (ppmoH, the analogue ligand for complex **3**) and 2,6-di(2-pyridyl)-4(1*H*)-pyridone (dppoH, the ligand for complex **5**) are given in the Supporting Information Figure S3. The spectrum of 4-chloro-2,2′:6′,2″-terpyridine (ctrpy) is also provided for comparison. It is clear that the influence of the middle ring is mainly reflected in the region of 310−375 nm. Although the UV−vis spectra of these ligands are different from 310 to 375 nm, they all provide the terdentate coordination. Therefore, in the electronic absorption spectra of their corresponding platinum complexes, they all exhibit the broad, low-energy charge transfer absorption band (Supporting Information Figure S3). The difference is that the energy of this band is influenced by the lowest unocuppied molecular orbital (LUMO) of the terdentate ligand.

Emission Spectra. Complexes **2**−**5** are emissive in solution at room temperature and 77 K. The emission spectra of **2**−**5** in acetonitrile are displayed in Figure 4, and the emission data are presented in Tables 1 and 2. The emission energy of **2** and **4** at room temperature is quite similar, while the emission of **3** appears at a somewhat higher energy in comparison to those of **2** and **4**. In contrast, the emission of **5** occurs at a much lower energy compared to those of **2**−**4**, which is in line with its red-shifted MLCT band in the electronic absorption. In comparison to their corresponding excitation spectra, **2**−**5** all exhibit a Stokes shift of approximately 140 nm. The lifetimes of **2**, **4**, and **5** are all around 1 μs, whereas the lifetime of **3** is unable to be detected because of the weak signal in acetonitrile at room temperature. Similar to other reported platinum complexes,[1a−d,g] the long emission lifetimes (except **3**) and large Stokes shift of **2**−**5** suggest that the emitting state of these complexes could be ascribed to a ^{3}MLCT state in nature. Although the emission energy does not change in the concentration range of 5.0×10^{-6} to 5.0×10^{-5} mol/L for **2**, **4**, and **5**, and the emission intensity keeps increasing in this concentration range (see Supporting Information Figure S4 for **4**), the emission lifetimes of **2**, **4**, and **5** decrease with increased concentration. The decreased lifetime at higher concentrations could emanate from self-quenching, which is commonly seen in transition-metal complexes including platinum(II) complexes.[1a,17] The self-quenching rate constants are obtained from the slope of the decay rate constant versus complex concentration plot, and the results are listed in Table

(16) Liu, X.-J.; Feng, J.-K.; Meng, J.; Pan, Q.-J.; Ren, A.-M.; Zhou, X.; Zhang, H.-X. *Eur. J. Inorg. Chem.* **2005**, 1856.

(17) (a) Lai, S. W.; Chan, M. C. W.; Cheung, T. C.; Peng, S. M.; Che, C. M. *Inorg. Chem.* **1999**, *38*, 4046. (b) Büchner, R; Cunningham, C. T.; Field, J. S.; Haines, R. J.; McMillin, D. R.; Summerton, G. C. *J. Chem. Soc., Dalton Trans.* **1999**, 711. (c) Kunkely, H.; Vogler, A. *J. Am. Chem. Soc.* **1990**, *112*, 5625. (d) Wan, K.-T.; Che, C.-M.; Cho, K.-C. *J. Chem. Soc., Dalton Trans.* **1991**, 1077. (e) Hissler, M.; Connick, W. B.; Geiger, D. K.; McGarrah, J. E.; Lipa, D.; Lachicotte, R. J.; Eisenberg, R. *Inorg. Chem.* **2000**, *39*, 447.

Table 1. Photophysical Parameters of **2**−**5**

complex	λ_{abs}/nm (ε/M^{-1} cm^{-1})	λ_{em}/nm (τ_{em}/ns; k_q/M^{-1} s^{-1})[a] R.T.	λ_{em}/nm[b] 77 K	$\lambda_{T1\text{-}Tn}$/nm (ε/M^{-1} cm^{-1}; τ_{TA}/ns)[c]	Φ_T
2	217 (5.18×10^4), 248 (4.85×10^4), 267 (4.58×10^4), 430 (8.50×10^3)	564 (960; 1.6×10^{10})	526 564	480 (-; 540), 725 (2274; 500)	0.37
3	230 (3.22×10^4), 282 (1.68×10^4), 353 (4.12×10^3), 405 (5.79×10^3)	556 (31; −)	530 564	460 (1161; 33), 690	0.46
4	218 (4.14×10^4), 253 (3.98×10^4), 267 (4.05×10^4), 423 (7.40×10^3)	563 (1300; 5.4×10^9)	522 554	480 (-, 890), 725 (1715; 880)	0.21
5	285 (2.18×10^4), 310 (1.38×10^4), 324 (1.51×10^4), 445 (6.24×10^3)	585 (1200; 5.1×10^9)	553 633	380 (-; 910), 482 (-; 940), 770 (1428, 1095)	1.00

[a] Measured in CH_3CN for **2**−**4**, and in 1:1 (v/v) CH_3CN:DMSO for **5**. The τ_{em}'s listed are the intrinsic lifetime τ_0 at the infinitely dilute concentration. [b] Measured at a complex concentration of 1.0×10^{-5} mol/L in butyronitrile. [c] Measured at a complex concentration of 6.2×10^{-5} mol/L for **2** and 8.0×10^{-5} mol/L for **4** in CH_3CN, 9.5×10^{-5} mol/L for **3** and 1.4×10^{-4} mol/L for **5** in DMSO.

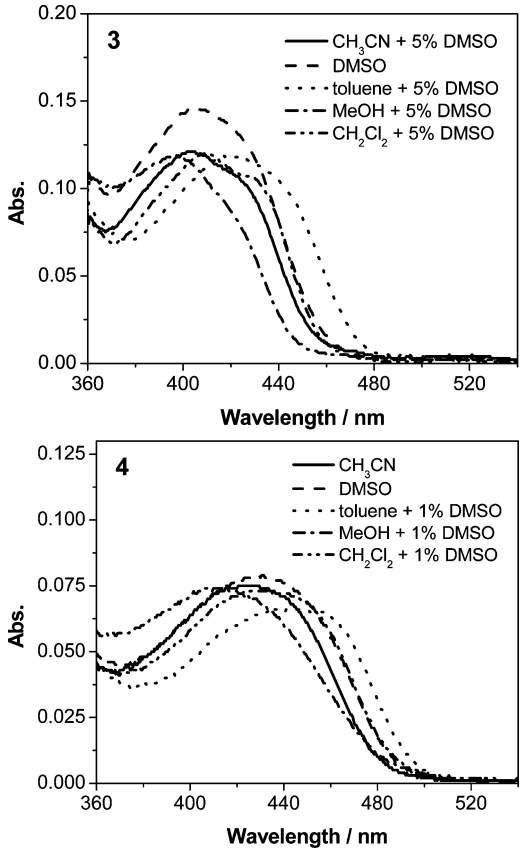

Figure 3. Electronic absorption spectra of complexes **3** and **4** in different solvents. The complex concentration is 2.5×10^{-5} mol/L for **3**, and 1.0×10^{-5} mol/L for **4**.

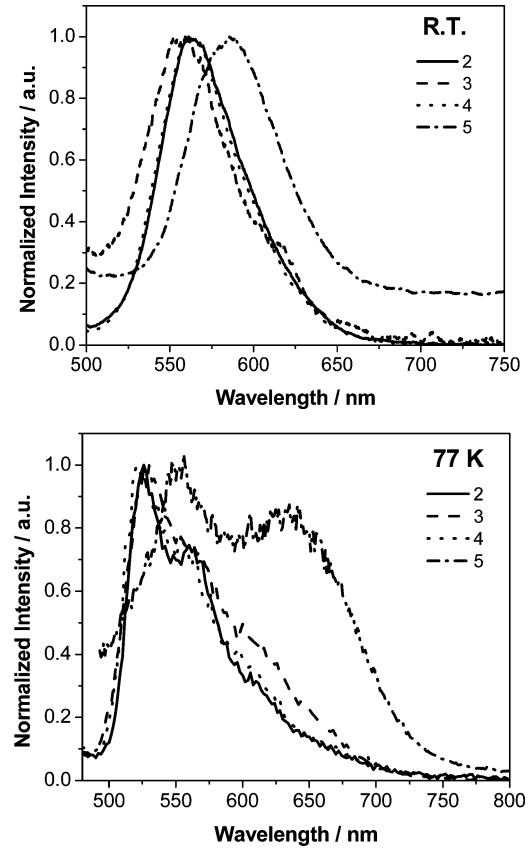

Figure 4. Normalized emission spectra of complexes **2**−**5** in acetonitrile solutions at room temperature (the solution of **5** contains 4% DMSO) and in butyronitrile glassy solution at 77 K. The complex concentration is 1.0×10^{-5} mol/L at room temperature and 2.0×10^{-5} mol/L at 77 K. The excitation wavelength is 425 nm for **2**, 415 nm for **3**, 423 nm for **4**, and 445 nm for **5**.

1 for **2**, **4**, and **5**, which are several times larger than those of platinum terpyridyl complexes.[1a]

Similar to the UV−vis absorption, the emission of **2**−**4** also exhibits solvent dependence. As shown in Figure 5 for complex **4**, the emission energy decreases in low-polarity solvents. This indicates that the emitting excited state is less polar than the ground state, which is in line with the attribution of the emitting state to the ^{3}MLCT state. The emission quantum yields of **2**−**4** are quite distinct in different solvents (Table 2). In general, these complexes are more emissive in dichloromethane and acetonitrile than in DMSO and methanol.

In butyronitrile glassy solution at 77 K, **2**−**4** exhibit blue-shifted emissions and vibronic structures with a spacing of approximately 1200 cm^{-1} (Figure 4), which corresponds to the aromatic vibronic mode of the terdentate ligand. Unlike the emission at room temperature, the emission energy of **2**−**4** at 77 K is quite similar. In contrast, the emission of **5** at 77 K appears at lower energies with a spacing of ∼2285 cm^{-1} between the two bands. With reference to the emission of other reported platinum(II) terpyridyl complexes,[1a,4b] the emission of **2**−**5** at 77 K could be tentatively assigned to the ^{3}MLCT excited state as well.

Triplet Transient Difference Absorption. As shown in Figure 6 and Supporting Information Figure S5, **2** and **4** exhibit similar time-resolved triplet transient different absorption spectra from 370 to 820 nm in acetonitrile, with one band appearing at ∼480 nm and another extending from 520 to 820 nm with a band maximum at ∼725 nm. For **3**, because of the limited solubility in acetonitrile, it is dissolved in DMSO. In comparison to those of **2** and **4**, the TA band maxima for **3** blue-shifts to ∼460 nm and ∼690 nm, respectively. Nevertheless, the TA spectra of these three complexes exhibit positive absorption from the near-UV to near-IR region, suggesting that the triplet excited-state absorption of **2**−**4** is stronger than that of the ground state

Table 2. Emission Quantum Yields and Lifetimes (ns, in Parenthesis) of **2**−**5** in Different Solvents

complex	CH_3CN	DMSO	Toluene[b]	MeOH[b]	CH_2Cl_2 [d]
2	0.044 (950)	0.004 (120)	0.033 (20, 68%; 540, 32%)	0.009 (190)	0.063 (1630)
3	0.003	0.002 (20)	0.021 (26, 13%; 735, 87%)	*c*	0.020 (340)
4	0.060 (1300)	0.007 (160)	0.011 (120, 8%; 2970, 92%)	0.017 (150)	0.120 (2400)
5	0.044 (1200)[a]				

[a] In CH_3CN/DMSO (v/v 1:1). [b] For **3**, with ∼5% DMSO; for **2** and **4**, with ∼1% DMSO. [c] Too weak to be detected. [d] For **2** and **3**, with ∼5% DMSO. **4** is in pure dichloromethane.

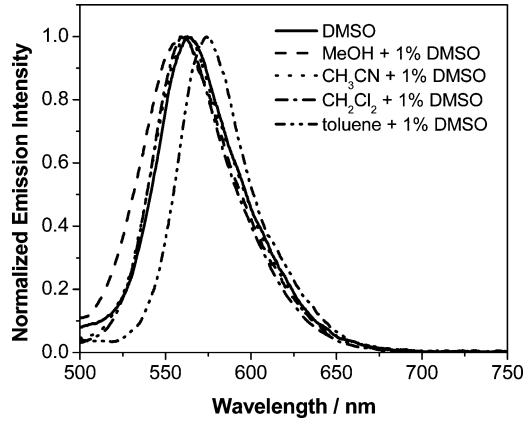

Figure 5. Normalized emission spectra of complex **4** in different solvents. Excitation wavelength = 423 nm, concentration = 1.0×10^{-5} mol/L.

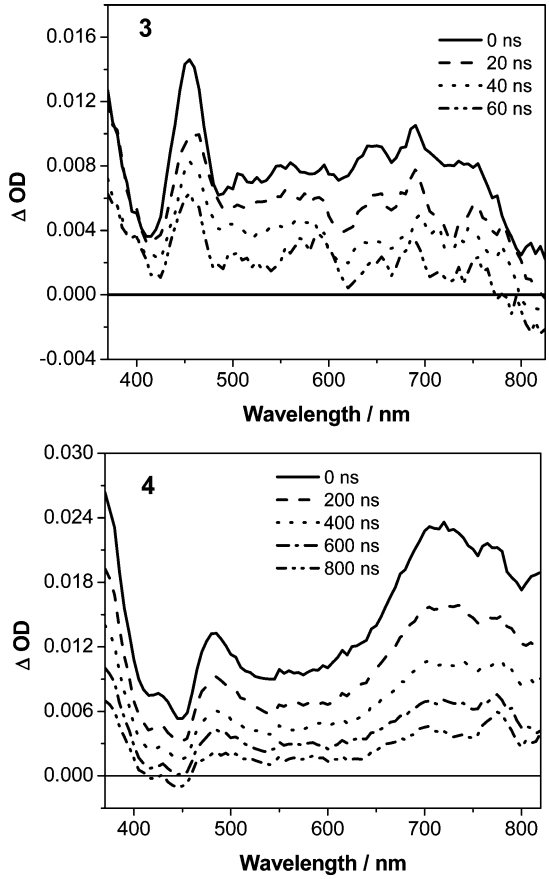

Figure 6. Time-resolved triplet transient difference absorption spectra of **3** and **4** in argon-degassed solutions at room temperature following 355 nm excitation. The time indicated in the figures is the time delay after excitation. The solvent is DMSO for **3**, and acetonitrile for **4**. The complex concentration is 9.5×10^{-5} mol/L for **3** and 8.0×10^{-5} mol/L for **4**.

in this region. The shape of the TA spectrum of **5** resembles that of **3** at the visible region, but is similar to those of **2** and **4** in the near-IR region with a band maximum appearing at 770 nm. The lifetimes obtained from the decay of the transient absorption for **2**, **4**, and **5** essentially coincide with those obtained from the time-resolved emission measurement at the same concentration (see Supporting Information Figure S6 for complex **4**), indicating that the transient absorption could arise from the same excited state that emits, that is, the ^{3}MLCT transition. This assignment is consistent with what has been reported by Castelleno and co-workers for platinum terpyridyl complexes.[18]

The triplet excited-state absorption coefficients of **2** and **4** at 725 nm are of the same order; with the $\varepsilon_{T1\text{-}Tn}$ of **4** is 33% larger than that of **2**. The triplet quantum yield (Φ_T) of **4** is 76% higher than that of **2**. In contrast, the $\varepsilon_{T1\text{-}Tn}$ of **3** at 460 nm is much smaller than those of **2** and **4** at 725 nm. However, the quantum yield of the triplet excited-state formation of **3** doubles that of **2** and is 11% higher than that of **4**. The larger Φ_T but a shorter triplet excited-state lifetime for **3** compared to those of **2** and **4** suggests that the nonradiative decay rate constant of the triplet excited state of **3** is much higher than those of **2** and **4**. This could be attributed to the closer energy gap between the ^{3}MLCT state and the nonradiative ^{3}d,d state in **3** compared to that in **2** and **4**, in which the electron-donating 4-ethynyltolyl ligand lowers the energy of the ^{3}MLCT/^{3}LLCT state.[5b]

Acid-Response. Complexes **2**−**4** all exhibit acid-dependent photophysical properties. Figure 7 shows the UV−vis spectral change of **3** and **4** in acetonitrile upon addition of *p*-toluenesulfonic acid. With increased *p*-toluenesulfonic acid concentration, the low energy charge-transfer band of **3** at 405 nm gradually decreases, while the band at 376 nm increases until 1 equiv of acid is added. Well-defined isosbestic points at 238, 283, 293, 327, 352, and 387 nm suggest that only two absorbing species are present in the solution, that is, **3** and its corresponding protonated complex. A similar phenomenon has been observed for **2** and **4** (see Figure 7 and Supporting Information Figure S7), with isosbestic points appearing at approximately 237, 294, 326, 352, 389, and 462 nm. However, the changes in the charge-transfer bands of **2** and **4** are somewhat different from that of **3**. For **3**, the whole charge transfer band blue-shifts upon addition of acid; while for **2** and **4**, the charge transfer band becomes broader, accompanied by the increased absorption between 352 and 389 nm, the decrease of the portion between 389 and 462 nm, and the increase of the tail above 462 nm. These differences could be attributed to the different compositions of ^{1}MLCT and ^{1}LLCT in **2**, **4**, and **3**. In **3**, the

(18) Shikhova, E.; Danilov, E. O.; Kinayyigit, S.; Pomestchenko, I. E.; Tregubov, A. D.; Camerel, F.; Retailleau, P.; Ziessel, R.; Castellano, F. N. *Inorg. Chem.* **2007**, *46*, 3038.

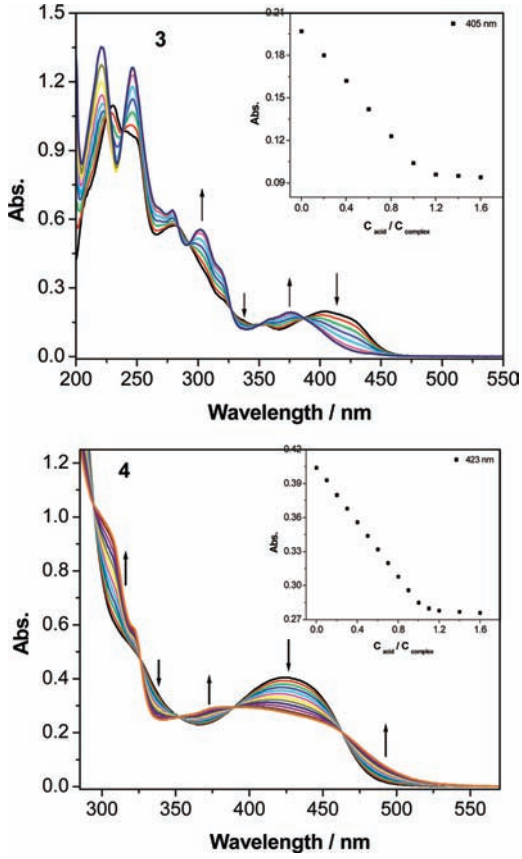

Figure 7. UV−vis absorption spectral changes of **3** ($c = 3.4 \times 10^{-5}$ M) and **4** ($c = 5.0 \times 10^{-5}$ M) in acetonitrile with increasing *p*-toluenesulfonic acid concentration. Inset: Plot of absorbance vs [$C_{acid}/C_{complex}$] at 405 nm for **3** and at 423 nm for **4**.

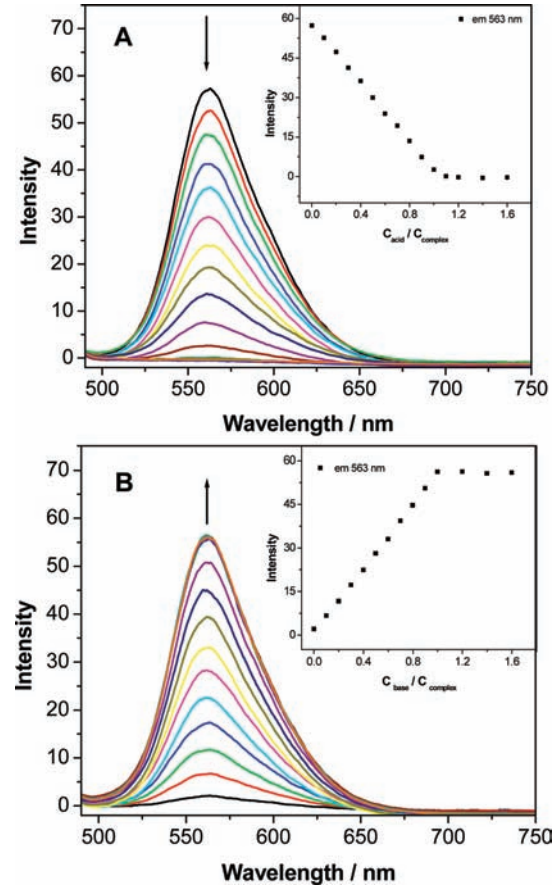

Figure 8. (A) Emission spectra of of **4** ($c = 5.0 \times 10^{-5}$ M) in acetonitrile with increasing *p*-toluenesulfonic acid concentration. Inset: Plot of relative emission intensity vs [$C_{acid}/C_{complex}$] at 563 nm. (B) Emission spectra of **4** ($c = 5.0 \times 10^{-5}$ M) + 1 equiv of *p*-toluenesulfonic acid in acetonitrile with increasing triethylamine concentration. Inset: Plot of relative emission intensity vs [$C_{base}/C_{complex}$] at 563 nm.

dominant contributor to the charge-transfer band is ^{1}MLCT transition because of the poor electron-donating ability of Cl. In contrast, the charge-transfer bands in **2** and **4** have contributions from both ^{1}MLCT and ^{1}LLCT transitions. The ^{1}MLCT transition shifts to a high energy for the protonated species of the complexes, which will be further discussed in the last paragraph of the Results and Discussion section. On the other hand, the relative contribution of the ^{1}MLCT and ^{1}LLCT transitions to the charge-transfer bands of the protonated forms of **2** and **4** could be different from that in the original forms. Increased contribution from the ^{1}LLCT transition would cause the increase of the tail above 462 nm.

The acid−based UV−vis spectral changes of **2**−**4** are completely reversible upon addition of bases, such as triethylamine. Supporting Information Figure S8 shows the electronic absorption spectral changes upon base titration of the acetonitrile solutions of **3** and **4** with 1 equiv of *p*-toluenesulfonic acid. After addition of 1 equiv of triethylamine, the spectrum is fully recovered to its original shape. The reversibility of the UV−vis spectral changes for these complexes is confirmed by alternating addition of 1 equiv of *p*-toluenesulfonic acid and 1 equiv of triethylamine. Within 10 repeating cycles, the spectral changes are reproducible.

Emission responses of **2**−**4** to acid were also investigated in acetonitrile solutions. All three complexes exhibit dramatic emission intensity decrease upon addition of *p*-toluenesulfonic acid. The emission is completely quenched when 1 equiv of *p*-toluenesulfonic acid is added. No variations in the emission energy or the shape of the emission spectrum are observed during the acid-titration process. Figure 8A presents the quench of the emission of **4** in acetonitrile upon acid titration. Complexes **2** and **3** exhibit a similar feature. The quench of the emission intensity upon acid titration should be attributed to the protonation of **4**, which will be further discussed in the following paragraphs. Similar to the reversible change of the UV−vis spectrum upon base addition, the emission intensity change is also fully reversible by adding triethylamine to the acidified solutions. As exemplified by **4** in Figure 8B, upon triethylamine addition, the emission is returned-on. With increasing amount of triethylamine added to the solution, the emission intensity at 563 nm keeps increasing until 1 equiv of triethylamine is added. At this point, the spectrum is recovered to the original shape and intensity and remains unchanged with further base addition. The emission turn-off and return-on procedure is highly reproducible; the original emission feature is retained even after ten repeating cycles of alternating addition of 1 equiv of *p*-toluenesulfonic acid and triethylamine.

In addition to the UV−vis absorption and emission spectra, the triplet transient difference absorption spectra of **2**−**4** also

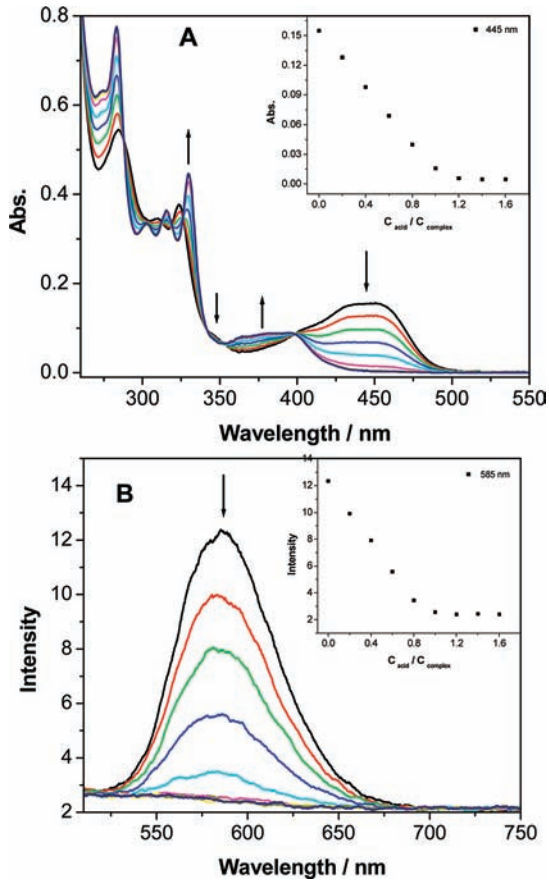

Figure 9. (A) UV−vis absorption spectral changes of **5** ($c = 2.5 \times 10^{-5}$ M) in acetonitrile + 5% DMSO with increasing *p*-toluenesulfonic acid concentration. Inset: Plot of absorbance vs [$C_{acid}/C_{complex}$] at 445 nm. (B) Emission spectra changes of **5** ($c = 2.5 \times 10^{-5}$ M) in acetonitrile + 5% DMSO with increasing *p*-toluenesulfonic acid concentration. Inset: Plot of relative emission intensity vs [$C_{acid}/C_{complex}$] at 585 nm.

exhibit acid-dependence. When *p*-toluenesulfonic acid is added to the acetonitrile solutions of **2**−**4**, the intensity of the transient absorption is drastically reduced. Upon addition of 1 equiv of *p*-toluenesulfonic acid, the transient absorption disappears. However, the transient absorption can be recovered when triethylamine is added to the acidified solutions.

The acid-dependent UV−vis absorption, emission, and transient absorption of **2**−**4** could be attributed to the protonated forms of these complexes. Because both carbonyl oxygen and the 3-nitrogen on the pyrimidin-4-one ring have lone pair(s) of electrons, it is possible that either the oxygen or the nitrogen atom could be protonated. To figure out which atom is protonated, complex **5** that contains the pyridin-4-one ring instead of the pyrimidin-4-one ring was synthesized, and its acid-dependent UV−vis and emission spectra were investigated. Because of the limited solubility of **5** in acetonitrile, **5** was dissolved in DMSO and diluted with acetonitrile in our studies. As shown in Figure 9A, with increased *p*-toluenesulfonic acid concentration, the low-energy band of the UV−vis spectrum of **5** at 445 nm decreases, while the band around 380 nm increases, and clear isosbestic points at 398, 354, 342, 326, 319, and 288 nm are observed. In addition, the emission band at about 585 nm is gradually quenched upon acid addition (Figure 9B). Similar to what has been observed for **2**−**4**, the acid-dependent

Scheme 2

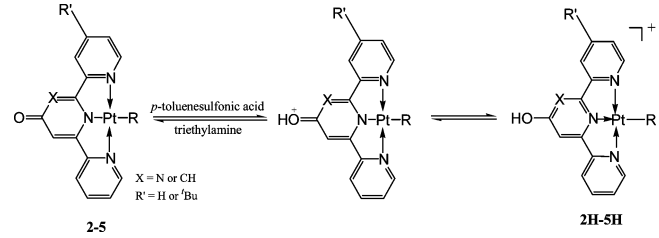

absorption and emission of **5** is reversible. Upon addition of 1 equiv of triethylamine to the acidified solution, both the UV−vis absorption and the emission spectra are fully recovered to their original features (see Supporting Information Figure S10). Because of the absence of 3-nitrogen on the pyridin-4-one ring, protonation can only occur at the carbonyl oxygen. Considering the similar spectroscopic changes in **2**−**4** to those in **5** upon addition of acid or base, we conclude that the protonation of **2**−**4** also occurs at the carbonyl oxygen.

Upon protonation of **2**−**5**, the tautomerization indicated in Scheme 2 could occur. Because of the electron-donating ability of the OH substituent, the terdentate ligand based LUMO would be destabilized, which results in an increased energy gap between the Pt or Pt/C≡C-tolyl based highest occupied molecular orbital (HOMO). As a result, the ^{1}MLCT band in the UV−vis absorption spectrum is blue-shifted. In addition, the electron-rich hydroxyl substituent could cause photoinduced electron transfer (PET) from the hydroxyl substituent to the platinum center, which would quench the ^{3}MLCT emission. When triethylamine is added to the acidified solution, deprotonation of **2H**−**5H** occurs, which converts them back to the original **2**−**5** form and the original spectroscopic features are recovered. The protonation of the carbonyl oxygen in **2**−**5** is further supported by the ^{1}H NMR spectral changes of **2**−**5** under acidic condition. As exemplified by complex **5** in Figure 1, upon addition of 0.2−0.6 equiv of CF_3CO_2H acid, the ^{1}H NMR peaks for H_a-H_e all shift to downfield and become broadened. The broadening of the NMR signal should be attributed to the mixture of the original form and the protonated form of **5**. When 0.8 equiv of CF_3CO_2H is added, the splitting patterns are able to be observed again. Upon addition of 1 equiv of CF_3CO_2H, the NMR spectrum of **5** becomes identical to that of **5a**, except that the chemical shift of H_a appears at a slight downfield. Addition of excess amount of CF_3CO_2H causes minor changes on the peaks of H_b − H_e, while the H_a peak further downfield shifts. This indicates that the protonated form of **5** has the same structure as **5a**. The downfield shift of H_a's could be due to the formation of hydrogen bonds between the excessively added CF_3CO_2H and the hydroxyl hydrogen in the protonated form of **5**, which could reduce the electron density on the nearby hydrogens, that is, H_a's, and thus causes the downfield shift. Additional evidence supporting the identical structure of the protonated form of **5** to that of **5a** comes from the identical UV−vis absorption spectra and the similar IR spectra for the protonated form of **5** to that of **5a** (Supporting Information Figures S11 and S1, respectively).

Conclusion

The photophysical studies of complexes **2**−**5** reveal that they all exhibit solvent-dependent ^{1}MLCT or ^{1}MLCT/^{1}LLCT electronic absorption and ^{3}MLCT emission at room temperature and 77 K. **2**−**5** also possess broadband triplet excited-state absorption from the near-UV to near-IR spectral region. The triplet excited-state lifetime is around 1 μs for **2**, **4**, and **5**. Most importantly, their photophysical properties are influenced drastically by acid. Upon addition of acids, the original ^{1}MLCT or ^{1}MLCT/^{1}LLCT band intensity decreases with an increase of the band at about 380 nm. The emission and the triplet transient absorption are gradually quenched after acidification. These changes are fully reversible by adding bases to the acidified solution. The acid-dependent photophysics of **2**−**5** could be attributed to the protonation and deprotonation of the carbonyl oxygen.

Acknowledgment. Acknowledgment is made to the National Science Foundation (CAREER CHE-0449598) for financial support. We are also grateful to North Dakota State EPSCoR (ND EPSCoR Instrumentation Award) for support.

Supporting Information Available: The IR spectra of **5**, **5a** and **5**+HCl, the electronic absorption spectra of **2** in different solvents, the electronic absorption spectra of three ligands and their corresponding Pt(II) chloride complexes, the concentration-dependent emission spectra of **4** in CH_3CN at room temperature, the time-resolved triplet transient difference absorption spectra of **2** and **5**, the emission and TA decays curves of **4**, the reversible UV−vis absorption and emission spectral changes of **2**, **3**, **4**, and **5** upon addition of acid or base, and the electronic absorption spectra of **5a** and protonated **5**. This material is available free of charge via the Internet at http://pubs.acs.org.

IC801919G